Expression of Synaptic and Phototransduction Markers During Photoreceptor Development in the Marmoset Monkey *Callithrix jacchus*

ANITA HENDRICKSON[1,2], **DAVID TROILO**[3], **HIDAYAT DJAJADI**[1], **DANIEL POSSIN**[2], and **ALAN SPRINGER**[4,*]

[1]Department of Biological Structure, University of Washington, Seattle, Washington 98195

[2]Department of Ophthalmology, University of Washington, Seattle, Washington 98195

[3]SUNY College of Optometry, New York, New York 10036

[4]New York Medical College, Valhalla, New York 10595

Abstract

Marmoset photoreceptor development was studied to determine the expression sequence for synaptic, opsin, and phototransduction proteins. All markers appear first in cones within the incipient foveal center or in rods at the foveal edge. Recoverin appears in cones across 70% of the retina at fetal day (Fd) 88, indicating that it is expressed shortly after photoreceptors are generated. Synaptic markers synaptophysin, SV2, glutamate vesicular transporter 1, and CTBP2 label foveal cones at Fd 88 and cones at the retinal edge around birth. Cones and rods have distinctly different patterns of synaptic protein and opsin expression. Synaptic markers are expressed first in cones, with a considerable delay before they appear in rods at the same eccentricity. Cones express synaptic markers 2–3 weeks before they express opsin, but rods express opsin 2–4 weeks before rod synaptic marker labeling is detected. Medium/long-wavelength-selective (M&L) opsin appears in foveal cones and rod opsin in rods around the fovea at Fd 100. Very few cones expressing short-wavelength-selective (S) opsin are found in the Fd 105 fovea. Across peripheral retina, opsin appears first in rods, followed about 1 week later by M&L cone opsin. S cone opsin appears last, and all opsins reach the retinal edge by 1 week after birth. Cone transducin and rod arrestin are expressed concurrently with opsin, but cone arrestin appears slightly later. Marmoset photoreceptor development differs from that in *Macaca* and humans. It starts relatively late, at 56% gestation, compared with *Macaca* at 32% gestation. The marmoset opsin expression sequence is also different from that of either *Macaca* or human.

Indexing terms

retina; opsin; cones; rods; arrestin; transducin; synaptophysin; recoverin

---

The New World common marmoset monkey (*Callithrix jacchus*) has several practical advantages over Old World *Macaca* monkeys for experimental investigation of primate retinal development. Their smaller size, rapid maturation, and more frequent breeding with multiple births provide significant cost and time savings when studying primate retinal

---

*Correspondence to: Alan Springer, PhD, Department of Cell Biology and Anatomy, New York Medical College, Valhalla, NY 10595. E-mail: springer@nymc.edu.

development. In a previous paper (Hendrickson et al., 2006), we showed that the marmoset retina and its vasculature have a spatial developmental pattern that is identical to previous morphological descriptions of fetal and infant macaque and human retinal development (Hendrickson and Kupfer, 1976; Provis et al., 1985, 1998; Yuodelis and Hendrickson, 1986; Packer et al., 1990; LaVail et al., 1991; Hendrickson and Drucker, 1992; Hendrickson, 1992; Dorn et al., 1995; Bumsted et al., 1997; Georges et al., 1999; Xiao and Hendrickson, 2000; Provis, 2001; Springer and Hendrickson, 2004; Hendrickson and Provis, 2006).

The one marked difference between macaque and marmoset is in the temporal development of the fovea, the specialized region responsible for high visual acuity. At birth, the marmoset fovea is relatively immature compared with a macaque neonate, but it then undergoes a rapid postnatal development with foveal morphology, suggesting that the fovea may be mature within 8–12 weeks (wk) postnatally (Hendrickson et al., 2006). This is much faster than macaque monkey fovea development, which takes 12–15 months to reach adult cone density and pit morphology (Hendrickson and Kupfer, 1976; Packer et al., 1990), or human fovea development, which takes 4–6 years (Hendrickson and Yuodelis, 1984; Yuodelis and Hendrickson, 1986). If confirmed by ongoing quantitative measures, this rapid postnatal development in marmosets significantly shortens the time required to reach a mature endpoint in experimental studies of eye growth, amblyopia, and emmetropization.

Many studies in humans and macaque monkeys (for review see Hendrickson and Provis, 2006) and our recent study in marmoset (Hendrickson et al., 2006) have emphasized that developmental differentiation/maturation begins first in the incipient foveal region and ends weeks to months later in the far peripheral retina. For instance, cones within the macaque fovea express synaptic markers at fetal day (Fd) 55–60 (Okada et al., 1994), just days after the fovea is first detected morphologically (Hendrickson, 1992), but these same markers do not appear in far peripheral cones until Fd 125–135. Macaque cone opsins, synaptic proteins, and phototransduction proteins (Sears et al., 2000) and human synaptic proteins, opsins, and photoreceptor transcription factors (Georges et al., 1999; Milam et al., 2000; Xiao and Hendrickson, 2000; Swain et al., 2001; Bumsted O'Brien et al., 2004) all show a similar early central to later peripheral expression pattern. These findings indicate that central cones are forming functional synapses with bipolar and/or horizontal cells at an early stage of retinal development, but this process takes many weeks to be completed across the peripheral retina. Given the relatively rapid late fetal and neonatal development of marmoset fovea (Hendrickson et al., 2006), we predict that spatial-temporal expression patterns for major photoreceptor proteins might also occur relatively late in gestation. This was tested by using well-characterized antisera for immunocytochemical labeling of primate retina. Our results show that all proteins are expressed in a temporal/spatial sequence similar to that of macaque, but with their expression initiated relatively late in gestation. Surprisingly, the marmoset temporal opsin sequence is different from that of either macaque or humans.

MATERIALS AND METHODS

Tissue processing

All tissue was obtained under approved University of Washington Institutional Animal Care Committee protocols from tissue programs at San Antonio Primate Center, Wisconsin Regional Primate Center, and New England College of Optometry. Marmoset monkeys included in this study were Fd 75 (n = 1), Fd 88 (n = 2), Fd 100–110 (n = 3), Fd 125 (n = 2 twins), Fd 133–135 (n = 3 triplets), postnatal (P) 0.5–2 days (n = 8), P 7–10 days (n = 4), P 1 month (n = 2), P 2–4 months (n = 4), P 6–8 months (n = 2), and adults 3 years or older (n = 4). Details of tissue processing are the same as described previously (Hendrickson et al., 2006).

Primary antibodies

All primary antibodies, their working dilutions, the immunogen used in their generation, and their sources are listed in Table 1. For each antibody, all immunolabeling patterns reported in this study conform to previous results in human, macaque, or marmoset retina published from this laboratory or to other published results cited below.

The mouse monoclonal antibody (mab) against the endothelial cell membrane protein platelet-endothelial adhesion molecule 1 or CD31 has been characterized in Western blots (No. M0823; Dako, Santa Barbara, CA) as being a 130-kDa transmembrane glycoprotein. The antigen was human spleen. Immunolabeling has shown that CD31 is expressed in endothelial cells of many species. CD31 labeling patterns have been described previously in marmoset retinal blood vessels (Hendrickson et al., 2006) and are identical to those shown in this paper.

The mab against cone arrestin (CAr; gift of C. Craft, University of Southern California, Los Angeles) was originally generated by immunization of mice with *Macaca* monkey retinal extracts (Wikler et al., 1997). Winkleer et al. found that the 7G6 antibody immunolabeled the outer segment, cell body cytoplasm, and synapse of primate cones. Recently, the 7G6 antibody was characterized by proteolytic digestion and peptide immunoprecipitation as recognizing N-terminal amino acids 98–388 of human cone arrestin (Zhang et al., 2003). Our use of 7G6 to label cones in developing primate retina has been described (Swain et al., 2001).

The mab against the alpha subunit of cone transducin (CTr; gift of J. Hurley, University of Washington, Seattle) recognizes a 40.5-kDa band in Western blots of human retina and immunolabels the outer segments and cytoplasm, including the synapse of primate cones (Lerea et al., 1989).

The mab against C-terminal binding protein 2 (CTBP2), a RIBEYE homologue, recognizes a 48-kDa protein in Western blots of rat retina according to its source (No. 612044; BD Biosciences, Heidelberg, Germany). As previously shown in macaque and marmoset retina, CTBP2 labels ribbons in photoreceptor and bipolar cell synaptic terminals (tom Dieck et al., 2005; Jusuf et al., 2006).

The rabbit polyclonal antibody against glutamate vesicular transporter 1 (GluVT1) was raised against a Strep-tag fusion protein containing amino acid residues 456–560 of rat GluVT1 and recognizes a 60-kDa protein in Western blots of rat brain (No. 135302; Synaptic Systems, Göttingen, Germany). It localizes to retinal photoreceptor and bipolar cell ribbon-containing synaptic terminals (Mimura et al., 2002; Sherry et al., 2003).

The rabbit polyclonal antibody against medium- and long-wavelength-selective (M&L) cone opsin was generated to 18 amino acids of the carboxy terminal of human M cone opsin (Lerea et al., 1989) and recognizes a 38-kDa band in Western blots of human retina (Saari, unpublished observations). This antiserum labels both M and L primate cones, because of the similarity between their opsin amino acid sequences. It shows high specificity for M&L opsin in both fetal and adult retina and has been used previously in our laboratory to study human and macaque cone development (Bumsted et al., 1997; Xiao and Hendrickson, 2000).

The rabbit polyclonal antibody against recoverin (Rec) was raised against recombinant human protein and recognizes a 25-kDa protein on Western blots of mouse retina (AB5585; Chemicon, Temecula, CA). This calcium-binding protein has been detected only in

photoreceptors and midget bipolar cells of retina, including primates (Milam et al., 1993; Haverkamp et al., 2003).

The mab against rod opsin (4D2; gift of R. Molday, University of British Columbia, Vancouver) was generated to a rat outer segment membrane preparation. Further characterization by proteolytic digestion and peptide immunoprecipitation showed that 4D2 recognizes amino acids 2–39 of the N-terminal region of rod opsin (Hicks and Molday, 1986). We have used 4D2 to label primate retina (Dorn et al., 1995).

The rabbit polyclonal antibody to rod arrestin (RAr; gift of C. Craft, University of Southern California, Los Angeles) was generated to amino acids 287–296 of bovine rod arrestin and its specificity documented by immunolabeling of baboon rod outer segments at the light and electron microscopic level (Nir and Ransom, 1992). In Western blots of bovine retina, this antibody recognizes a 48-kDa protein, characteristic of the arrestin 1/S antigen/rod arrestin group of the arrestin superfamily (Craft and Whitmore, 1995).

The rabbit polyclonal antibody JH455 to S cone opsin (gift of J. Nathans, Johns Hopkins University, Baltimore) was generated to 48 amino acids at the carboxy end of human S opsin (Wang et al., 1992). Immunolabeling with JH455 in primates marks 8–10% of the cones, and the resulting topography revealed by JH455 documents that it recognizes S cone opsin in both fetal and adult primate retina (Bumsted et al., 1997; Martin and Grunert, 1999; Xiao and Hendrickson, 2000).

The mab to synaptic vesicle protein 2 (SV2; gift of K. Buckley, Harvard Medical School, Boston) recognizes a 78-kDa transmembrane glycoprotein in synaptic vesicles of neurons and endocrine cells (Buckley and Kelly, 1985). This monoclonal antibody recognizes isoforms A, B, and C of SV2 (Bajjalieh, 1999). At the electron microscopic level, SV2 is found in synaptic vesicles of both conventional and ribbon synapses in macaque retina (Okada et al., 1994).

The mab to synaptophysin (Synap) detects a 38-kDa protein on Western blots of rat brain and labels neurons, neuromuscular junctions, paracrine cells, and neuronal tumors of all mammalian species according to its source (S5768; Sigma-Aldrich, St. Louis, MO). At the EM level, Synap labels photoreceptor and bipolar cell synaptic terminals in primate retina (Koontz and Hendrickson, 1993).

Immunocytochemical labeling

Paraffin sections within, or adjacent to, the fovea were dewaxed in xylene, hydrated through descending alcohols to 0.01 M phosphate-buffered saline (PBS; pH 7.4), and then reacted in 3.3% Revealit in distilled water (Immunosolutions.com; a gift from David Pow, University of Newcastle, Newcastle, Australia) overnight at 37°C to retrieve antigenicity. After a brief rinse in PBS, slides were dried on a 37°C hotplate for 5 minutes and blocked for 1 hour in 10% Chemiblocker (Millipore Corp., Billerica, MA) in diluent (0.5% Triton X-100 and 0.05% azide in PBS). Frozen sections were washed in PBS and blocked as described above. All sections were then incubated overnight in a mixture of primary antiserum generated in rabbit, mouse, or rat in diluent containing 5% Chemiblocker. Details regarding primary antisera are given in Table 1. On the following morning, slides were washed for 3×20 minutes in PBS and incubated for 1 hour in the dark in a mixture of antirabbit IgG/Alexa 488 and antimouse IgG/Alexa 594 (Molecular Probes, Eugene, OR), each diluted 1/500 in diluent. Slides were washed for 3×20 minutes in PBS and coverslipped with Polymount (Polysciences, Willmington, PA). Whole-mount labeling times were extended to overnight for block, 3–5 days for primary, 2–3 days for wash, and 4–6 hours for secondary.

Data analysis

All analysis was done on sections through the developing fovea and comparisons used serial sections of the same retina. A mixture of monoclonal and polyclonal antibodies was used for double labeling to compare spatial and temporal expression of two proteins. Some sections were imaged and analyzed with a Nikon microscope equipped with narrowband fluorescence filters, photographed with Kodak Ekta-chrome 200ASA daylight film, and digitized with a Microtek scanner. Selected sections were imaged with a Zeiss LSM two-photon confocal microscope. Whole mounts were digitally imaged using a Nikon E1000 wide-field digital microscope. All images were processed in Adobe Photoshop CS3 for color balance, sharpness, and contrast.

RESULTS

Morphological appearance of the outer and inner plexiform layers

A brief review of the morphological development of the marmoset retina is presented here to help the reader understand the following immunocytochemical labeling patterns. The temporal development of the outer nuclear (ONL; i.e., photoreceptor layer), outer plexiform (OPL), inner nuclear (INL), inner plexiform (IPL), and ganglion cell (GCL) layers at the foveal edge, where rods first appear from Fd 100 to birth, is shown in Figure 1A–D. Figure 1E–H shows development in the nasal midperiphery from Fd 125 to 1 month postnatally. Fd 88 was the youngest fetus displaying a fovea (not shown), defined as the only region in temporal retina that contained five layers. The foveal ONL contained a very thin OPL underlying a single layer of flat, wide cones. Rods could not be identified at this age.

The fovea at Fd 100 (Fig. 1A) contains a single layer of wide, short cones and a thicker OPL and IPL, and scattered rods are present on the edge as a second, inner layer of small, dense cell bodies (Fig. 1A, arrows). By Fd 125 (Fig. 1B), cones are more numerous, and, by Fd 135 (Fig. 1C), both short outer (OS) and inner (IS) segments are present. In contrast, the nasal midperipheral retina is still quite immature at Fd 125 (Fig. 1E). A distinct GCL and a thin IPL are present, but the outer retina consists only of a thick outer neuroblastic layer (OnbL) in which large cones at the retinal edge are the only neurons that can be identified (Fig. 1E, arrow). Development occurs rapidly, so that, by Fd 135, a thick ONL is set off from the INL by a thin IPL (Fig. 1F, arrow).

At birth (Fd 143–144), cones on the foveal edge (Fig. 1D) are several layers thick, with a single deeper layer of rods. The inner edge of the OPL is bordered by a prominent band of cone pedicles. Both rods and cones have formed elongated axons called the "fibers of Henle" (FH). The FH angle away from the developing foveal pit and fibers in the IPL also show a similar slant, reflecting the onset of laminar displacements associated with pit formation (Hendrickson and Kupfer, 1976;Provis et al., 1998;Hendrickson et al., 2006;Hendrickson and Provis, 2006). By birth, the midperipheral ONL (Fig. 1G) contains distinct cones and rods with short IS and OS, and other retinal layers look quite mature. Over the next months, parafoveal photoreceptor OS and IS become much longer, and the numbers of cone nuclei in the foveal center and rod nuclei on the slope increase with age as rods are displaced centrally as cones pack (see Hendrickson et al., 2006). In the periphery (Fig. 1H), all layers become thinner with age as the retina is stretched by postnatal eye growth (Springer and Hendrickson, 2005). Peripheral photoreceptor OS and IS progressively elongate, at least to 3 months after birth.

Temporal expression of synaptic proteins, opsins, and recoverin in photoreceptors

Fetal day 88—Despite the morphological immaturity of the Fd 88 incipient fovea, the IPL and cones are labeled (+) for SV2 (Fig. 2A), Synap (Fig. 2C), CTBP2 (not shown), and

GluVT1 (Fig. 2E). The IPL is labeled more heavily than cones for SV2 and Synap (Fig. 1A), whereas cone pedicles label more heavily for GluVT1 than BP terminals in the IPL (Fig. 2E). Cone labeling for SV2, Synap, and GluVT1 is cytoplasmic and occurs throughout the cell at this age. CTBP2 labeling at the cone base and cytoplasm is punctate. In the Fd 88 central retina, all cones are heavily Rec$^+$ (Fig. 2B,D), and lightly Rec$^+$ cones extend beyond SV2$^+$ or Synap$^+$ cones into the periphery (Fig. 2A,B, arrowheads). Rods are not labeled for Rec at this age. This absence suggests that peripheral progenitors have adopted the cone phenotype but have not yet begun to express synaptic markers. Rec$^+$ cones >1 mm outside the fovea have complex, branched processes that extend from the basal future synaptic region into the inner retina, with some reaching the IPL (Fig. 2F). Short remnants of these basal processes are still present on central cones, including in the incipient fovea (Fig. 2C,D arrow). Similar processes on ferret rods and cones make transient contacts in the IPL and then retract with age (Johnson et al., 1999). Opsins were not detected at Fd 88.

Fetal days 105–115—In the Fd 100–105 incipient fovea, GluVT1 (Fig. 3A), SV2 (not shown), and Synap (Fig. 3C) heavily label cone cytoplasm, and CTBP2 (Fig. 3B) prominently labels ribbons in the cone pedicles. Outside the fovea, both rods and cones, based on their position in the ONL, are Rec$^+$ (Fig. 3E), and both cones and rods label for SV2 (Fig. 3F). Some SV2$^+$ or Synap$^+$ processes can be traced from cones to the IPL (Fig. 3F, arrowheads), but at many points label is absent between basal processes and ONL, suggesting that many processes near the IPL are BP axons. Rec labeling of putative rods can be detected no farther than 1 mm from the foveal edge. In contrast, Rec$^+$ cones (Fig. 3G), which also are lightly SV2$^+$ (Fig. 3H), are present into the far peripheral retina, despite the absence of an identifiable OPL or ONL at this eccentricity (Fig. 3J). These different expression patterns indicate that cones express Rec and synaptic proteins well before rods.

M&L and rod opsins (4D2) are all present in, or around, the Fd 100–105 incipient fovea (Figs. 4, 5A,B). All foveal cones were Synap$^+$ (Fig. 3C), whereas only a few were M&L$^+$ (Fig. 3D, arrows), suggesting that M&L opsin is first expressed between Fd 90 and Fd 95. In whole mounts (Fig. 4), the Fd 105 incipient fovea is surrounded by many 4D2$^+$ rods, which delineate a 950-μm-wide central rod-free fovea. This rod-free "hole" is filled with M&L$^+$ cones, which are the only labeled cones in the retina. In contrast, 4D2$^+$ rods form a dense 350-μm-wide band around the fovea and then extend, at lower density, almost to the optic disc (Fig. 4). A single S$^+$ cone was detected within the incipient fovea at Fd 100, and only five S$^+$ cones were present in the Fd 105 fovea (not shown). Labeling of the cell membrane by opsin shows clearly the difference in cell size and shape between the smaller rods (red) and the larger, rounder cones (green) at this age (Fig. 5A, inset). Only a few of the many Rec$^+$ rods express opsin (Fig. 5B), supporting an earlier expression of Rec vs. opsin in rods. From Fd 105 onward, rods are rare within the incipient foveal center.

Fetal days 125–135—At Fd 125, a thick band of Rec$^+$ cones and rods extends to the edge of the retina (Fig. 6A, arrowhead), suggesting that progenitors have adopted the photoreceptor fate across the entire retina. By Fd 135, despite the morphological immaturity of peripheral retina (Fig. 1F), cone pedicles in the OPL <2 mm from both retinal edges are Synap$^+$ (Fig. 6B) as well as SV2$^+$ (not shown). Cone pedicle labeling before birth for CTBP2 and GluVT1 is prominent from central (Fig. 6C,D) into peripheral (Fig. 6E,F) retina. Despite the late expression of S opsin (see below), peripheral S$^+$ cones (Fig. 6G,H) have Synap$^+$ and CTBP2$^+$ pedicles shortly before birth, which are indistinguishable from surrounding M&L cones. It is more difficult to determine when the very small rod spherules contain synaptic markers. At Fd 135, near the optic disc, confocal imaging for M&L opsin (Fig. 6J,K) and CTBP2 (Fig. 6J,L) showed long CTBP2$^+$ presumptive rod ribbons (arrows) in unlabeled spaces above the large M&L$^+$ cone pedicles that were filled with multiple short CTBP2$^+$ ribbons (arrowheads). Although by Fd 135 short cone synaptic ribbons were

present into the far peripheral retina (Fig. 6C), it was difficult to identify the long rod ribbons beyond the optic disc until after birth.

In contrast to synaptic development, opsin expression at Fd 125 is still confined to central retina (Fig. 4). M&L$^+$ cones fill the foveal center and extend 800 μm into the temporal ONL and 1,200 μm into the nasal ONL, whereas 4D2$^+$ rods extend 2 mm beyond the foveal edge in the temporal and 4 mm in the nasal ONL (Figs. 4, 5C). The observation that 4D2 is detected more peripherally than M&L, indicates that rods express opsin before M&L cones. At Fd 125, S$^+$ cones were present across the foveal center (Fig. 5C, left), but only 500–700 μm into the periphery (Figs. 4, 5C), showing that S opsin covers a significantly smaller central area than M&L opsin. S cones were consistently detected within the fovea throughout development, although at a lower density than on the foveal edge. By Fd 135 (not shown) 4D2$^+$ rods are close to or at the nasal edge. M&L$^+$ cones are ~1 mm and S$^+$ cones are ~2 mm from the nasal edge. This sequence confirms an opsin expression pattern in marmoset of rod opsin before M&L opsin before S opsin.

P1–30 days—By birth, all synaptic markers were present in cone pedicles to the retinal edge (Fig. 6M). Staining intensity for synaptic markers increases over the first few postnatal weeks in the far periphery, probably because of the appearance of synaptic markers in the more numerous rod spherules. Rod ribbons were present far into the periphery by P10d.

At birth, the shallow foveal pit was overlain with a wide region of M&L$^+$ cones with 4D2$^+$ rods on the foveal edge (Fig. 5F). At higher magnification (Fig. 5G), the parafoveal rods have basal axons and tiny synaptic pedicles (arrows) that tilt away from the foveal pit, indicating that packing has started (Hendrickson and Kupfer, 1976). By birth, 4D2$^+$ rods extended to the retinal edge, but M&L$^+$ cones had not quite reached the edge (Fig. 6M, arrow). The most peripheral S$^+$ cones were still ~700 μm from the edge. By P10d, the diameter of the rod-free zone in the foveal center had decreased to ~500 μm (Fig. 5H), and M&L$^+$ cones were packed into the foveal center (Fig. 5J). A low density of S$^+$ cones continues to be present across the fovea (Fig. 5K). Their labeling also shows elongated FH that point away from the foveal center (Fig. 5K, inset).

All three photoreceptor types were labeled for opsin at the temporal edge by P1 week (Fig. 4) and slightly later at the dorsal and ventral retinal edges. It took until 1–2 months of age for the nasal retinal edges to have a density of cone and rod OS similar to that of adults, although OS were still relatively short. By 2 months, most cell membrane opsin labeling across the retina was gone from cones, and only the occasional rod was heavily labeled.

Relationship of the foveal avascular zone to opsin expression

Central blood vessels (BV) are forming the foveal avascular zone (FAZ; Figs. 5E, 7A, arrowheads) at Fd 125 (Hendrickson et al., 2006). At this age, the edge of the rod-free zone in the ONL overlaps the most central BV forming the FAZ in the GCL (Fig. 7B, arrowheads). However, this correlation does not continue, because at Fd 135 the FAZ is 175 μm in diameter (Fig. 7C), whereas the rod-free zone diameter still is 940–970 μm (Fig. 7D,R). In Fd 125, Fd 135, and P1d whole mounts, S$^+$ cones were distributed sparsely across the foveal center overlying the FAZ (Figs. 4, 5C left, E, inside arrows) and more densely outside it (Fig. 5C center, E left). Thus, the topography of neither rods nor S cones seems to correlate with FAZ diameter.

Temporal expression of phototransduction proteins in photoreceptors

Cones show cytoplasmic, but not nuclear, labeling for the alpha subunit of cone transducin (CTr; Lerea et al., 1989) with mab A1.1 throughout development. The earliest are detected

in the fovea at Fd 100–105 (Fig. 8A), when a minority of cones is outlined by M&L$^+$ membranes (Fig. 8A, arrowheads) and most contain CTr cytoplasmic labeling. CTr$^+$ cones extend for at least 300 μm beyond any M&L$^+$/CTr$^+$ cones, indicating that CTr is expressed shortly before opsin. In central cones at birth (Fig. 8C), cytoplasmic labeling for CTr extends throughout the cell and reveals the growth of the FH and the dramatic change in cell shape compared with Fd 105 (Figs. 2C,D, 8A). In contrast, OS labeling for CTr is detected after opsin is expressed, and the OS lengthens with increasing age. At birth, there is a narrow band of CTr$^+$ cones at the retinal edge (Fig. 8D, red arrowhead), just in front of CTr$^+$/M&L$^+$ cones (Fig. 8D, yellow arrowhead), which have heavily labeled M&L$^+$ OS. After birth, CTr cytoplasmic labeling increases in the FH and synaptic pedicle, and the OS becomes heavily CTr$^+$ (Fig. 8H).

Rod arrestin (RAr; Nir and Ransom, 1992), as detected by the polyclonal antibody C10C10, lightly labels both the rod nucleus and the cytoplasm on the Fd 105 foveal edge, where many rods are RAr$^+$/4D2$^+$ (Fig. 8B, yellow arrowheads), others are only RAr$^+$ (Fig. 8B, green arrowheads), and a very few are only 4D2$^+$ (Fig. 8B, red arrowheads). This diversity of labeling patterns suggests that these two proteins are expressed close together but not sequentially. In neonatal central retina (Fig. 8F), RAr is heavier in the rod nucleus than in the cytoplasm, but many rod OS are clearly RAr$^+$/4D2$^+$. At the retinal edge, there is a leading front of RAr$^+$ rods (Fig. 8G, green arrowhead) slightly beyond RAr$^+$/4D2$^+$ rods (Fig. 8G, yellow arrowhead). With increasing postnatal age, RAr increases in intensity throughout the cytoplasm, including the synaptic spherule, and nuclear labeling decreases markedly (Fig. 8J). In the rod OS, RAr labeling is lighter than for the cytoplasm and much lighter than 4D2 labeling. Presumed S cones have RAr$^+$ synaptic pedicles (Fig. 8J, arrow) and OS (Fig. 8J, arrowhead).

Cone arrestin (CAr; Zhang et al., 2003), as detected by mab 7G6, is very faint in the Fd 100–105 fovea but is clearly present at Fd 125. Both nuclear and cytoplasmic labelings are a striking early characteristic of CAr. By birth, M&L$^+$ cones across the retina are CAr$^+$, with heavy nuclear and cell cytoplasm labeling and a faint CAr$^+$ OS (Fig. 8E). Nuclear labeling fades after birth, so that by P3 months only the OS and entire cytoplasmic compartment are heavily labeled (Fig. 8K). The two cone types differ markedly for staining with mab 7G6. M&L$^+$ cone nuclei and cytoplasm label heavily throughout development (Fig. 8E,K). S cones show only faint nuclear labeling at birth (Fig. 8E, arrows) and then become labeled for CAr after birth (compare Fig. 8K,K1).

DISCUSSION

Six features of marmoset photoreceptor development were identified in this study. 1) All photoreceptor markers appear first within the incipient foveal center for cones or on its edge for rods. The first cone markers were detected at Fd 88, and they reach the retinal edge around birth. 2) Synaptic markers are expressed first in cones, with a considerable time lag before synaptic markers appear in rods at the same eccentricity. 3) Both M&L$^+$ and S$^+$ cones express synaptic markers 2–3 weeks before they express opsin. 4) Rods express opsin 2–4 weeks before synaptic marker labeling is consistently detected. 5) Opsin is expressed first by rods, followed about 1 week later by M&L cones, with S opsin appearing last. This sequence differs from that of either macaques or humans. 6) The phototransduction protein Rec is one of the first cone markers to appear. CTr, CAr, and RAr are expressed concurrently with opsin.

Developmental events occur first in the fovea

The slow central to peripheral nature of primate retinal development aids in unraveling developmental sequences (for review see Hendrickson et al., 2006; Hendrickson and Provis,

2006). In *Macaca* monkeys, the earliest cones are generated on Fd 33 in the fovea, whereas the last cones are generated almost 10 weeks later in the far periphery, on Fd 100–105 (LaVail et al., 1991). SV2 labels foveal cones at Fd 55 (Okada et al., 1994), about 3 weeks after the first cones are generated, and appears in far peripheral cones at about Fd 100. M&L opsin appears 2 weeks later, at Fd 70, in foveal cones (Bumsted et al., 1997) and reaches the nasal retinal edge at Fd 155–160. Protein expression in macaque cones takes 6 weeks for SV2 and 10 weeks for M&L opsin to cover the retina. This study shows that all marmoset markers also appear first in, or around, the fovea and then move slowly across the retina. Because M&L opsin labels relatively few foveal cones at Fd 100, it is probably first expressed at about Fd 95, with cones at the temporal and nasal retinal edges labeled by P1 week, a span of 8 weeks. M&L opsin coverage requires the same amount of time for macaque and marmoset despite the much smaller marmoset fetal eye. A common method to compare developmental events between species is percentage gestation (%G). The marmoset has a 143-day gestation, whereas macaques average 170 days. The initiation and completion times for marmoset M&L opsin expression are 66%G to 105%G, compared with 41%G to 85%G for macaque. Therefore, M&L opsin expression starts and finishes later in gestation for the marmoset.

We lack specific information on developmental sequences in very young marmoset retina, but such sequences are well documented in macaques and can be used to suggest times for the marmoset. The morphological emergence of the macaque fovea occurs at Fd 50 (Hendrickson, 1992), when cell generation is finished in this region (LaVail et al., 1991). Cone SV2 expression begins shortly after the fovea can first be identified (Okada et al., 1994). In the Fd 75 marmoset, there was no region that contained five layers, nor could a cone-rich region be identified. The Fd 88 marmoset fovea contained a region ~700 μm wide with five distinct layers and an ONL containing only cones. This appears morphologically comparable to humans at fetal week (Fwk) 11 and *Macaca* at Fd 50 (Hendrickson, 1992), the earliest ages in these species at which the fovea contains all five layers. Synaptic markers CTBP2, GluVT1, SV2, and Synap also were detected in the Fd 88 marmoset incipient fovea. This suggests that the five-layered fovea appears and synaptic proteins could be expressed in marmosets as early as Fd 82–85. This indicates that foveal emergence and synaptic initiation occur at 56%G in marmosets, which is much later than the 42%G in macaque. Our findings indicate that marmoset retinal differentiation is compressed into the last half of gestation.

Another developmental comparison between species uses caecal period (CP), which is conception to first eyelid opening (Robinson, 1991). In macaque, CP is 133 days, whereas, in marmoset, it is 143 days. Even using %CP, the initiation of marmoset retinal development begins at a later time; for instance, SV2 expression is at 41%CP in macaque and 56%CP in marmoset. This later onset in retinal developmental processes likely reflects a genuine, marked delay in marmoset early fetal gestation compared with macaque/human, with later stages pushed closer to, or after, birth. This may be due to the conception of twins or triplets, which is common in marmosets and rare in macaques (Phillips, 1976).

Cones make synapses before they express opsin

Double labeling clearly shows that marmoset cones contain synaptic markers before they express M&L or S opsin. Throughout development, a solid line of Synap[+], GluVT1^{+}, SV2^{+}, or CTBP2^{+} cone pedicles is present in the OPL about 500–700 μm more peripherally than M&L[+] or S[+] cones. Excitatory amino acid transporter is found in photoreceptors at Fwk 10, with Synap and VGluT appearing by Fwk 12 (Diaz et al., 2007). A slightly later expression of Synap at Fwk 14 suggests that apoptosis in bipolar cells correlates with the onset of synaptogenesis in cones (Georges et al., 1999). This suggests that survival depends on correct synaptic contact between cones and their multiple, but specific, types of bipolar

cells. Because opsin is not expressed until 1–2 weeks later (Xiao and Hendrickson, 2000), it does not appear to play a similar role in bipolar cell survival. Thus, it appears that both types of cones contain synaptic pedicles with vesicles and ribbons before they form an OS and express opsin. When marmoset cone-driven circuits are functionally active remains to be determined, but our labeling and morphological data strongly indicate that most marmoset cones are both light sensitive and synaptically capable by birth.

Rod spherules are small and difficult to discern, so it is uncertain when marmoset rods have synaptic proteins. Large rod ribbons appear on the foveal edge between Fd 100 and Fd 125 and reach the far periphery after birth. In contrast, rods first express opsin at Fd 95–100, and 4D2$^+$ rods are at the retinal edge before birth. EM studies of outer retina have noted that monkey cones have fairly mature synapses while nearby rods still lack obvious synaptic machinery (Okada et al., 1994). In humans, there is a 2–3-week difference between cone and rod EM synaptic formation (Hollenberg and Spira, 1973). We also estimate, based on markers, an interval of at least 3 weeks between opsin expression and synaptic ribbon formation in marmoset rods.

Marmosets have an opsin expression sequence different from that of humans or macaques

In macaques (Bumsted et al., 1997), S opsin$^+$ cones move across peripheral retina together with rod opsin, with both reaching the retinal edge about 2 weeks before M&L opsin, giving a sequence of rod and S opsins before M&L opsin. In humans (Xiao and Hendrickson, 2000), S$^+$ cones are detected 1 month before M&L$^+$ cones. Unpublished data on human rod opsin indicate that it slightly lags M&L expression (Hendrickson, unpublished observations), so in humans S opsin appears first, then M&L, and finally rod opsin. In this study, we found that M&L and rod opsins appear at the same time around the fovea, but rod always leads M&L expression in peripheral retina. S opsin consistently lags behind the others, giving a marmoset sequence of rod opsin before M&L opsin before S opsin. Quite surprisingly, this means that three different patterns are found for New World monkeys, Old World monkeys, and human primate groups. In most mammals that have been studied (for review see Xiao and Hendrickson, 2000), S opsin typically appears before M&L opsin. In marmosets, S$^+$ cones constitute 8% of the cone population, which is similar to the case in macaque and human (Wilder et al., 1996), although the density of all cone phenotypes is higher across most of the retina (Troilo et al., 1993). Marmosets and macaques have S cones within the fovea, whereas human fovea is S cone free (Bumsted and Hendrickson, 1999). Thus, there is no obvious explanation for the difference in primate expression patterns. Rather, these differences suggest that opsin expression is driven by molecular factors operating within and on each cell type, with little or no interaction between types.

Phototransduction protein expression is not correlated with opsin expression

Rec appeared very early, being present in cones across 70% of the Fd 88 retina, so Rec is present at least 2 weeks before opsin appears. Rec is detected in human photoreceptors at Fwk 13 (Yan and Wiechmann, 1997), 2 weeks before M&L opsin appears (Xiao and Hendrickson, 2000). In unpublished studies (Hendrickson, unpublished observations), Rec was detected in incipient foveal cones at Fwk 9. These data suggest that Rec may be expressed shortly after the progenitor becomes postmitotic and adopts the cone fate. CTr and RAr appeared slightly before opsin, whereas CAr appeared after M&L$^+$ cones were detected. These cone sequences are similar to those of macaque (Sears et al., 2000). The earliest labeling is in the nucleus and cytoplasm, which may be related to the onset of synaptic development. Despite being generally classified as OS phototransduction proteins, in postnatal photoreceptors, CTr, CAr, and RAr heavily labeled the synaptic pedicle and spherule at all ages. This may reflect a light-dependent OS/IS intracellular shift of CAr in

rods, which has not been observed in cones (Elias et al., 2004), or it may reflect an additional role in other cellular functions, such as synaptic transmission.

CONCLUSIONS

This study shows that synaptic, opsin, and phototransduction proteins are expressed in most photoreceptors many weeks before the photoreceptors were exposed to light at birth. Although no physiological recordings exist to show when synaptic transmission begins, these data and the IPL labeling in progress indicate that action potentials could be transmitted to central visual centers before birth. One function may be to segregate, organize, and refine nasal and temporal retinal axons in the lateral geniculate nucleus and its striate cortex projections, although the exact role of such early retinal activity is currently under debate (Cook et al., 1999; Chalupa, 2007).

Acknowledgments

LITERATURE CITED

Bajjalieh SM. Synaptic vesicle docking and fusion. Curr Opin Neurobiol. 1999; 9:321–328. [PubMed: 10395572]

Buckley K, Kelly RB. Identification of a transmembrane glycoprotein specific for secretory vesicles of neural and endocrine cells. J Cell Biol. 1985; 100:1284–1294. [PubMed: 2579958]

Bumsted K, Hendrickson A. Distribution and development of short-wavelength cones differ between *Macaca* monkey and human fovea. J Comp Neurol. 1999; 403:502–516. [PubMed: 9888315]

Bumsted K, Jasoni C, Szel A, Hendrickson A. Spatial and temporal expression of cone opsins during monkey retinal development. J Comp Neurol. 1997; 378:117–134. [PubMed: 9120051]

Bumsted O'Brien KM, Cheng H, Jiang Y, Schulte D, Swaroop A, Hendrickson AE. Expression of photoreceptor-specific nuclear receptor NR2E3 in rod photoreceptors of fetal human retina. Invest Ophthalmol Vis Sci. 2004; 45:2807–2812. [PubMed: 15277507]

Chalupa LM. A reassessment of the role of activity in the formation of eye-specific retinogeniculate projections. Brain Res Rev. 2007; 55:228–236. [PubMed: 17433447]

Cook PM, Prusky G, Ramoa AS. The role of spontaneous retinal activity before eye opening in the maturation of form and function in the retinogeniculate pathway of the ferret. Vis Neurosci. 1999; 16:491–501. [PubMed: 10349970]

Craft CM, Whitmore DH. The arrestin superfamily: cone arrestins are a fourth family. FEBS Lett. 1995; 362:247–255. [PubMed: 7720881]

Diaz CM, Macnab LT, Williams SM, Sullivan RK, Pow DV. EAAT1 and D-serine expression are early features of human retinal development. Exp Eye Res. 2007; 84:876–885. [PubMed: 17379211]

Dorn EM, Hendrickson L, Hendrickson AE. The appearance of rod opsin during monkey retinal development. Invest Ophthalmol Vis Sci. 1995; 36:2634–2651. [PubMed: 7499086]

Elias RV, Sezate SS, Cao W, McGinnis JF. Temporal kinetics of the light/dark translocation and compartmentation of arrestin and alpha-transducin in mouse photoreceptor cells. Mol Vis. 2004; 10:672–681. [PubMed: 15467522]

Georges P, Madigan MC, Provis JM. Apoptosis during development of the human retina: relationship to foveal development and retinal synaptogenesis. J Comp Neurol. 1999; 413:198–208. [PubMed: 10524333]

Haverkamp S, Haeseleer F, Hendrickson A. A comparison of immunocytochemical markers to identify bipolar cell types in human and monkey retina. Vis Neurosci. 2003; 20:589–600. [PubMed: 15088712]

Hendrickson A. A morphological comparison of foveal development in man and monkey. Eye. 1992; 6:136–144. [PubMed: 1624035]

Hendrickson A, Drucker D. The development of parafoveal and mid-peripheral human retina. Behav Brain Res. 1992; 49:21–31. [PubMed: 1388798]

Hendrickson A, Kupfer C. The histogenesis of the fovea in the macaque monkey. Invest Ophthalmol Vis Sci. 1976; 15:746–756. [PubMed: 822712]

Hendrickson, A.; Provis, J. Comparison of development of the primate fovea centralis. In: Sernagor, E.; Harris, B.; Wong, R., editors. Retinal development. Leiden: Cambridge University Press; 2006. p. 126-49.

Hendrickson AE, Yuodelis C. The morphological development of the human fovea. Ophthalmology. 1984; 91:603–612. [PubMed: 6462623]

Hendrickson A, Troilo D, Possin D, Springer A. Development of the neural retina and its vasculature in the marmoset *Callithrix jacchus*. J Comp Neurol. 2006; 497:270–286. [PubMed: 16705674]

Hicks D, Molday RS. Differential immunogold-dextran labeling of bovine and frog rod and cone cells using monoclonal antibodies against bovine rhodopsin. Exp Eye Res. 1986; 42:55–71. [PubMed: 2420630]

Hollenberg MJ, Spira AW. Human retinal development: ultrastructure of the outer retina. Am J Anat. 1973; 137:357–385. [PubMed: 4730460]

Johnson PT, Williams RR, Cusato K, Reese BE. Rods and cones project to the inner plexiform layer during development. J Comp Neurol. 1999; 414:1–12. [PubMed: 10494074]

Jusuf PR, Martin PR, Grunert U. Synaptic connectivity in the midget-parvocellular pathway of primate central retina. J Comp Neurol. 2006; 494:260–274. [PubMed: 16320234]

Koontz MA, Hendrickson AE. Comparison of immunolocalization patterns for the synaptic vesicle proteins p65 and synapsin I in macaque monkey retina. Synapse. 1993; 14:268–282. [PubMed: 8248851]

LaVail MM, Rapaport DH, Rakic P. Cytogenesis in the monkey retina. J Comp Neurol. 1991; 309:86–114. [PubMed: 1894769]

Lerea CL, Bunt-Milam AH, Hurley JB. Alpha transducin is present in blue-, green-, and red-sensitive cone photoreceptors in the human retina. Neuron. 1989; 3:367–376. [PubMed: 2534964]

Martin PR, Grunert U. Analysis of the short wavelength-sensitive ("blue") cone mosaic in the primate retina: comparison of New World and Old World monkeys. J Comp Neurol. 1999; 406:1–14. [PubMed: 10100889]

Milam AH, Dacey DM, Dizhoor AM. Recoverin immunoreactivity in mammalian cone bipolar cells. Vis Neurosci. 1993; 10:1–12. [PubMed: 8424920]

Milam AH, Hendrickson AE, Xiao M, Smith JE, Possin DE, John SK, Nishina PM. Localization of tubby-like protein 1 in developing and adult human retinas. Invest Ophthalmol Vis Sci. 2000; 41:2352–2356. [PubMed: 10892883]

Mimura Y, Mogi K, Kawano M, Fukui Y, Takeda J, Nogami H, Hisano S. Differential expression of two distinct vesicular glutamate transporters in the rat retina. Neuroreport. 2002; 13:1925–1928. [PubMed: 12395093]

Nir I, Ransom N. S-antigen in rods and cones of the primate retina: different labeling patterns are revealed with antibodies directed against specific domains in the molecule. J Histochem Cytochem. 1992; 40:343–352. [PubMed: 1372630]

Okada M, Erickson A, Hendrickson A. Light and electron microscopic analysis of synaptic development in *Macaca* monkey retina as detected by immunocytochemical labeling for the synaptic vesicle protein, SV2. J Comp Neurol. 1994; 339:535–558. [PubMed: 8144745]

Packer O, Hendrickson AE, Curcio CA. Developmental redistribution of photoreceptors across the *Macaca nemestrina* (pigtail macaque) retina. J Comp Neurol. 1990; 298:472–493. [PubMed: 2229476]

Phillips IR. The reproductive potential of the common cotton-eared marmoset (*Callithrix jacchus*) in captivity. J Med Primatol. 1976; 5:49–55. [PubMed: 818387]

Provis JM. Development of the primate retinal vasculature. Prog Ret Eye Res. 2001; 20:799–821.

Provis JM, Van Driel D, Billson FA, Russell P. Development of the human retina: patterns of cell distribution and redistribution in the ganglion cell layer. J Comp Neurol. 1985; 233:429–451. [PubMed: 3980779]

Provis JM, Diaz CM, Dreher B. Ontogeny of the primate fovea: a central issue in retinal development. Prog Neurobiol. 1998; 54:549–580. [PubMed: 9550191]

Robinson, SR. Development of the mammalian retina. In: Dreher, B.; Robinson, SR., editors. Neuroanatomy of the visual pathways and their development. Boca Raton, FL: CRC Press; 1991. p. 69-128.

Sears S, Erickson A, Hendrickson A. The spatial and temporal expression of outer segment proteins during development of *Macaca* monkey cones. Invest Ophthalmol Vis Sci. 2000; 41:971–979. [PubMed: 10752930]

Sherry DM, Wang MM, Bates J, Frishman LJ. Expression of vesicular glutamate transporter 1 in the mouse retina reveals temporal ordering in development of rod vs. cone and ON vs. OFF circuits. J Comp Neurol. 2003; 465:480–498. [PubMed: 12975811]

Springer AD, Hendrickson AE. Development of the primate area of high acuity. 2. Quantitative morphological changes associated with retina and pars plana growth. Vis Neurosci. 2004; 21:775–790. [PubMed: 15683563]

Springer AD, Hendrickson AE. Development of the primate area of high acuity, 3: temporal relationships between pit formation, retinal elongation and cone packing. Vis Neurosci. 2005; 22:171–185. [PubMed: 15935110]

Swain PK, Hicks D, Mears AJ, Apel IJ, Smith JE, John SK, Hendrickson A, Milam AH, Swaroop A. Multiple phosphorylated isoforms of NRL are expressed in rod photoreceptors. J Biol Chem. 2001; 276:36824–36830. [PubMed: 11477108]

tom Dieck S, Altrock WD, Kessels MM, Qualmann B, Regus H, Brauner D, Fejtova A, Bracko O, Gundelfinger ED, Brandstätter JH. Molecular dissection of the photoreceptor ribbon synapse: physical interaction of Bassoon and RIBEYE is essential for the assembly of the ribbon complex. J Cell Biol. 2005; 168:825–836. [PubMed: 15728193]

Troilo D, Howland HC, Judge SJ. Visual optics and retinal cone topography in the common marmoset (*Callithrix jacchus*). Vision Res. 1993; 33:1301–1310. [PubMed: 8333154]

Wang Y, Macke JP, Merbs SL, Zack DJ, Klaunberg B, Bennett J, Gearhart J, Nathans J. A locus control region adjacent to the human red and green visual pigment genes. Neuron. 1992; 9:429–440. [PubMed: 1524826]

Wikler KC, Rakic P, Bhattacharyya N, MacLeish PR. Early emergence of photoreceptor mosaicism in the primate retina revealed by a novel cone-specific monoclonal antibody. J Comp Neurol. 1997; 377:500–508. [PubMed: 9007188]

Wilder HD, Grünert U, Lee BB, Martin PR. Topography of ganglion cells and photoreceptors in the retina of a New World monkey: The marmoset *Callithrix jacchus*. Vis Neurosci. 1996; 13:335–352. [PubMed: 8737285]

Xiao M, Hendrickson A. Spatial and temporal expression of short, long/medium, or both opsins in human fetal cones. J Comp Neurol. 2000; 425:545–559. [PubMed: 10975879]

Yan XX, Wiechmann AF. Early expression of recoverin in a unique population of neurons in the human retina. Anat Embryol. 1997; 195:51–63. [PubMed: 9006715]

Yuodelis C, Hendrickson A. A qualitative and quantitative analysis of the human fovea during development. Vis Res. 1986; 26:847–855. [PubMed: 3750868]

Zhang H, Cuenca N, Ivanova T, Church-Kopish J, Frederick JM, MacLeish PR, Baehr W. Identification and light-dependent translocation of a cone-specific antigen, cone arrestin, recognized by monoclonal antibody 7G6. Invest Ophthalmol Vis Sci. 2003; 44:2858–2867. [PubMed: 12824223]
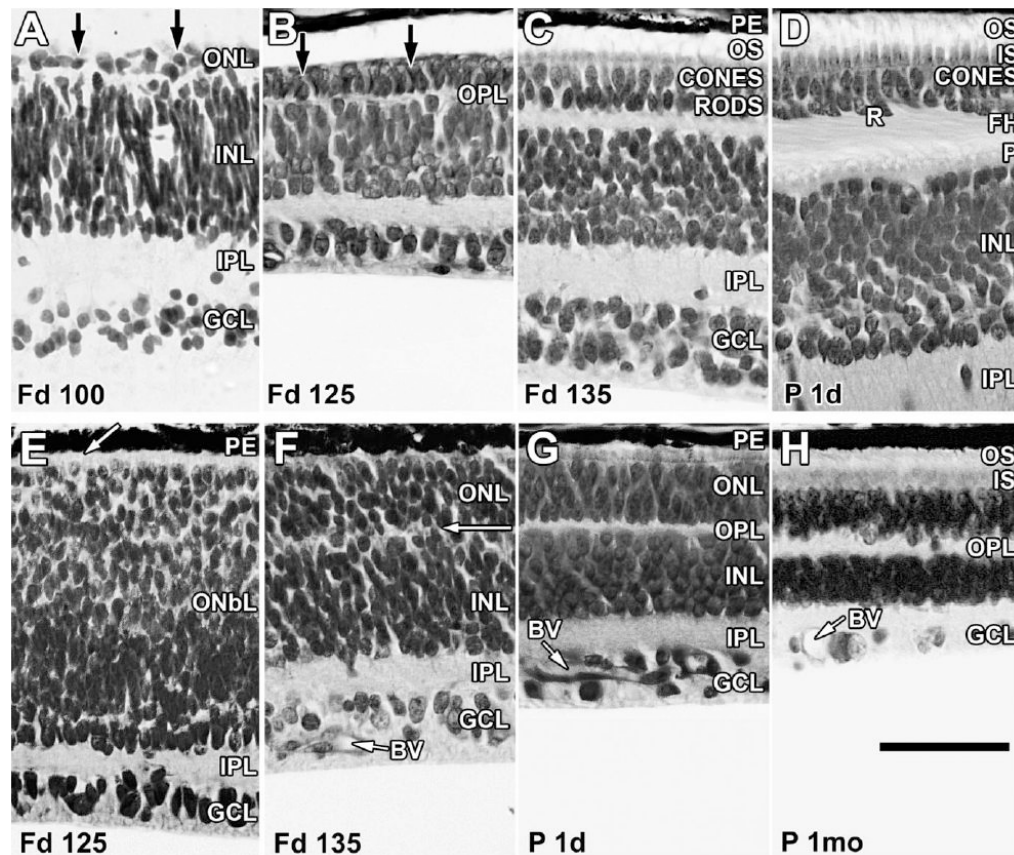
Figure 1.
Layer names and their abbreviations given in Figure 1 are used throughout the figure legends. Sections of marmoset retina at the foveal edge (A–D) and in the nasal midperiphery (E–H) stained with azure II and methylene blue. **A:** At Fd 100, the retina contains a distinct outer nuclear layer (ONL), a thin outer plexiform layer (OPL), a thick inner nuclear layer (INL), a thick inner plexiform layer (IPL), and a ganglion cell layer (GCL). The ONL contains cones and rods (arrows) but is still very thin. **B:** At Fd 125, the foveal edge has distinct cones and rods (arrows), and cell types are identifiable in INL. **C:** By Fd 135, the ONL contains more rods and is thicker because of the onset of cone and rod packing. Short outer segments (OS) are present. **D:** At birth, both rods (R) and cones have formed basal synaptic axons or FH, which tilt away from the foveal center (to the left), marking laminar displacement during pit formation. Both OS and inner segments (IS) are longer. The OPL is thicker, with a solid row of cone pedicles (P) lining its inner edge. Cones now are two or three deep, with rods intermixed between the cone FH. **E:** At Fd 125, the peripheral retina is markedly less mature than the central retina. The inner retina has a distinct IPL and GCL, but the outer retina is a thick neuroblastic layer (OnbL) in which only cones can be distinguished at the outer edge (arrow). **F:** By Fd 135, the ONbL is subdivided into ONL and INL by a thin, irregular OPL (arrow). Rods and cones are still difficult to identify in the ONL. Blood vessels (BV) in the GCL are growing across the peripheral retina. **G:** All layers are present in peripheral retina at birth, and BV have reached far peripheral retina. The ONL contains an outer layer of cones and a thick inner layer of rods that have short IS and OS in the interphotoreceptor space between the ONL and the pigment epithelium (PE). **H:** By 1 month, peripheral IS and OS are much longer, and the retina appears mature. Scale bar = 50 μm.
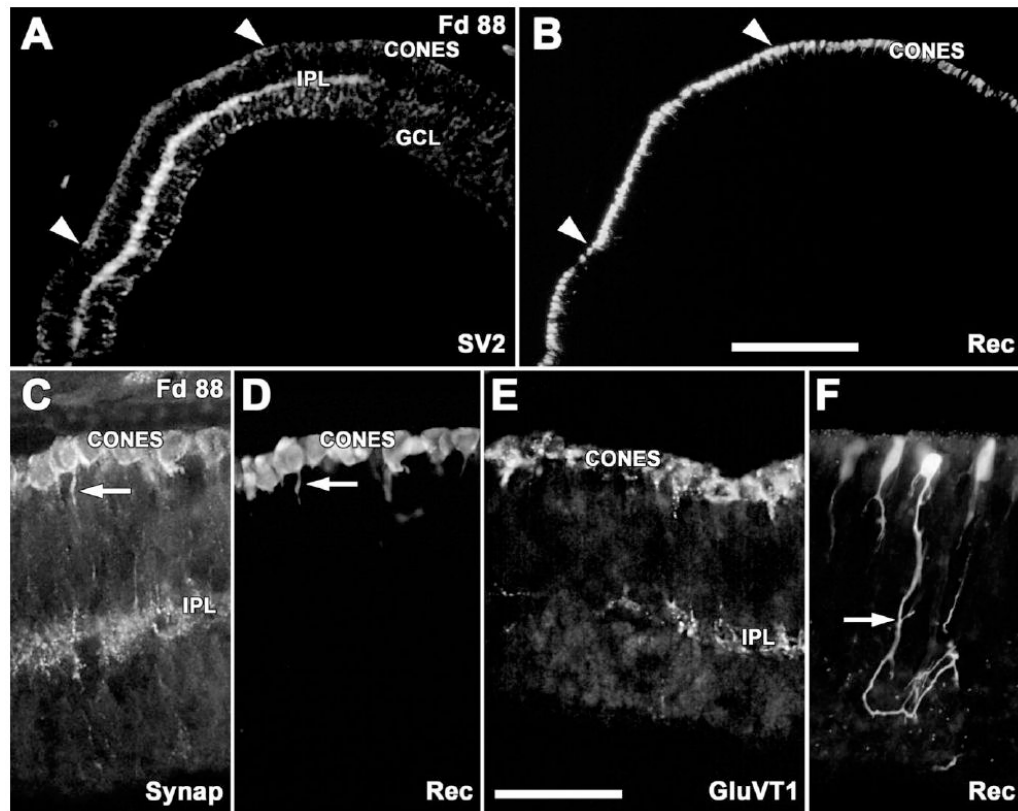
Figure 2.
Immunocytochemical labeling for early photoreceptor markers. **A,B:** Labeling in the fovea for the synaptic vesicle protein SV2 (A) and the calcium-binding protein recoverin (Rec; B). The IPL labels for SV2 slightly farther into the periphery than SV2 labeling in cones (arrowheads). Rec$^+$ cones are present well beyond the SV2$^+$ cones (arrowheads). **C,D:** Foveal cones are both synaptophysin$^+$ (Synap, A) and Rec$^+$ (D). Short processes (arrows) extend toward the SV2$^+$ IPL. **E:** Cones and the IPL on the foveal edge are glutamate vesicular transporter positive (GluVT1). Note basal processes on the cones. **F:** Outside of the fovea, immature Rec$^+$ cones have complex basal processes, which run into deeper retina (arrow). Scale bars = 200 μm in B (applies to A,B); 50 μm in E (applies to C–F).
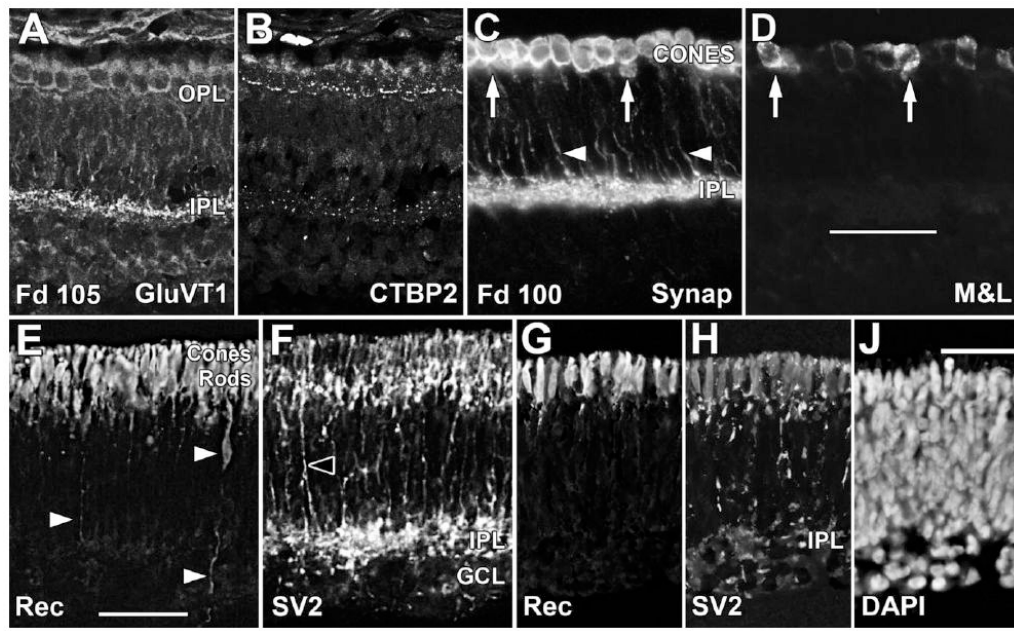
Figure 3.
Immunocytochemical labeling showing the expression of synaptic proteins at Fd 100–105.
A–D: The Fd 105 fovea shows OPL and IPL labeling for GluVT1 (A), synaptic ribbon
marker CTBP2 (B), and Synap (C). All foveal cones are heavily labeled for synaptic
markers, but only a few contain medium- and long-wavelength-selective cone opsin (M&L;
D, arrows). **E,F:** Near the optic disc, the outer retina contains a band of Rec+ cones and a
thick deeper band of Rec+ rods (E). At this eccentricity, there is a SV2+ IPL but no distinct
OPL (F), although the outer retina contains many cells that are SV2+. A few Rec+ (E, white
arrowheads) and many SV2+ processes (F, black arrowheads) extend into the deeper retina.
G–J: Near the retinal edge, there is a single layer of Rec+ cones (G), which are lightly SV2+
(H). SV2+ processes run into the SV2+ IPL. J: DAPI labeling shows the thin, irregular IPL
but no OPL. Scale bars = 50 μm in D (applies to A–D); 50 μm in E (applies to E,F); 20 μm
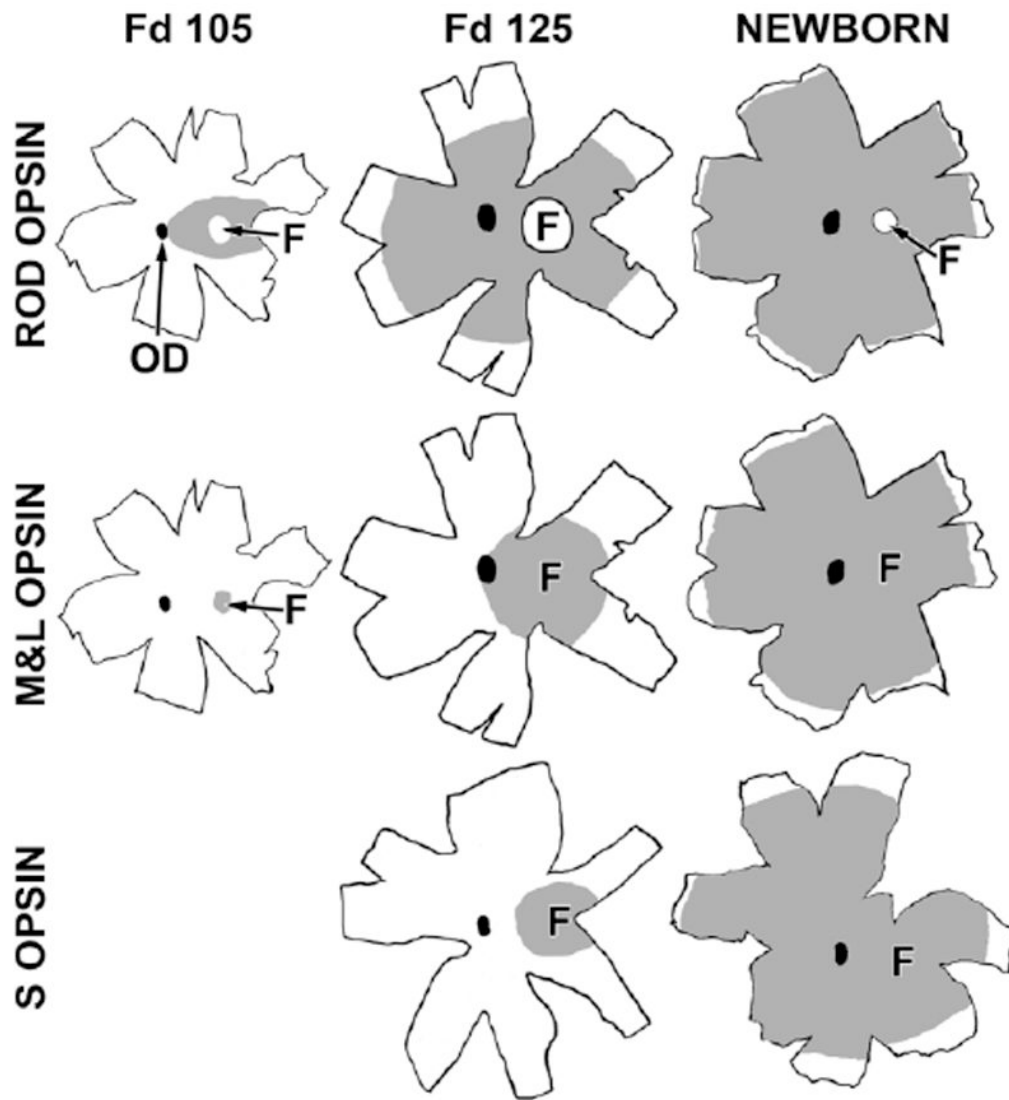in J (applies to G–J).

Figure 4.
Drawings of marmoset retinal whole mounts immunocytochemically labeled for rod opsin (top row), M&L cone opsin (middle row), and short-wavelength-selective (S) cone opsin (bottom row). The optic disc (OD) is the black oval in each drawing. The gray shading is the region containing labeled photoreceptors at each age. Rod opsin covers the central retina at Fd 105, with the exception of the fovea (F, indicated by the arrow). By Fd 125, rod opsin covers 70% of the retina, and, at birth, many rods near the retinal edge are labeled. Note that the fovea remains rod-free throughout development and that it becomes smaller with age. M&L opsin at Fd 105 is present only in the foveal cones. By Fd 125, M&L$^+$ cones fill the central retina to the OD, and, at birth, M&L opsin is near, but not at, the retinal edge. In contrast, at Fd 105, very few S opsin$^+$ cones were detected within the fovea (not shown). By Fd 125, S opsin was present only in and around the fovea and was still relatively far from the edge at birth. Scale bar = 5 mm.
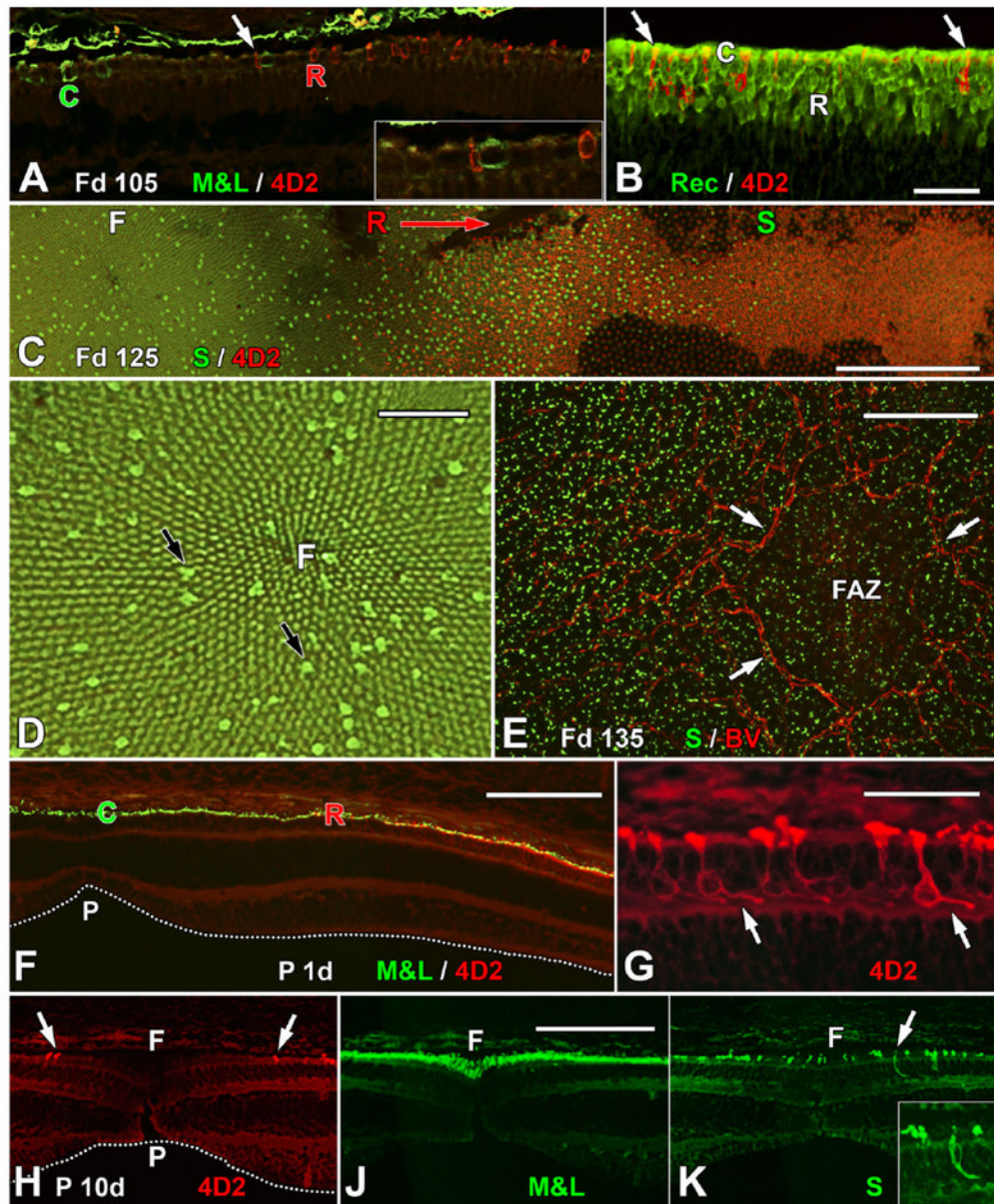
Figure 5.
Immunocytochemical labeling showing the expression of cone and rod opsins. **A:** The edge of the Fd 105 incipient fovea, showing the first M&L$^+$ cones (C) and rhodopsin$^+$ (4D2) rods (R). Note that both types of opsin$^+$ photoreceptors are scattered and not adjacent to one another. The region indicated by the arrow is shown at higher magnification in the inset. A small 4D2$^+$ red rod is adjacent to a larger thicker M&L$^+$ green cone. Note that opsin labeling is mainly in the cell membrane and tiny OS. **B:** The edge of 4D2 expression near the optic disc at Fd 105. Many rods (R) are Rec$^+$, whereas only a few have 4D2 (arrows). **C:** A Fd 125 whole mount comparing S opsin and 4D2 expression. The fovea (F, left) contains an irregular mosaic of S$^+$ cones that extends for >1.5 mm outside the fovea (S). The first rods (R) appear on the foveal edge. Many 4D2$^+$ rods are present into the periphery (direction of arrow), and 4D2$^+$ rods extend for at least 3 mm to the right of the picture edge. This pattern demonstrates that rod opsin is expressed in advance of S opsin. **D:** Higher magnification

view of the fovea in C. The foveal cone mosaic radiates from the foveal center (F). S$^+$ cones (black arrows) are irregularly scattered throughout the more numerous smaller M&L cones. **E:** Blood vessels (BV) forming the foveal avascular zone (FAZ; arrows) outline the incipient fovea. S$^+$ cones are present at low density within the FAZ and at higher density outside it. **F:** At birth, the immature foveal pit (P) is shallow and wide (dotted line). Overlying the pit, M&L$^+$ cones (C) form a single layer that extends for 400–450 μm to where the first 4D2$^+$ rods (R) appear. **G:** The 4D2$^+$ rods on the neonatal foveal edge have short FH (arrows) that point away from the foveal center, marking bipolar cell displacements in the INL associated with pit formation. **H,J:** Serial sections through the P10d fovea showing that the pit now is broader (H, dotted line) and the most central 4D2$^+$ rods (arrows) are >200 μm from the foveal center (F). M&L$^+$ cones are packed into the foveal center, forming a central multilayered ONL (J). S$^+$ cones extend across the foveal center (**K**). These also have FH that point away from the foveal center (inset). A magenta-green copy is available as Supporting Information Figure 1. Scale bars = 50 μm in B (applies to A,B); 500 μm in C; 100 μm in D,E; 200 μm in F; 50 μm in G; 100 μm in J (applies to H–K).
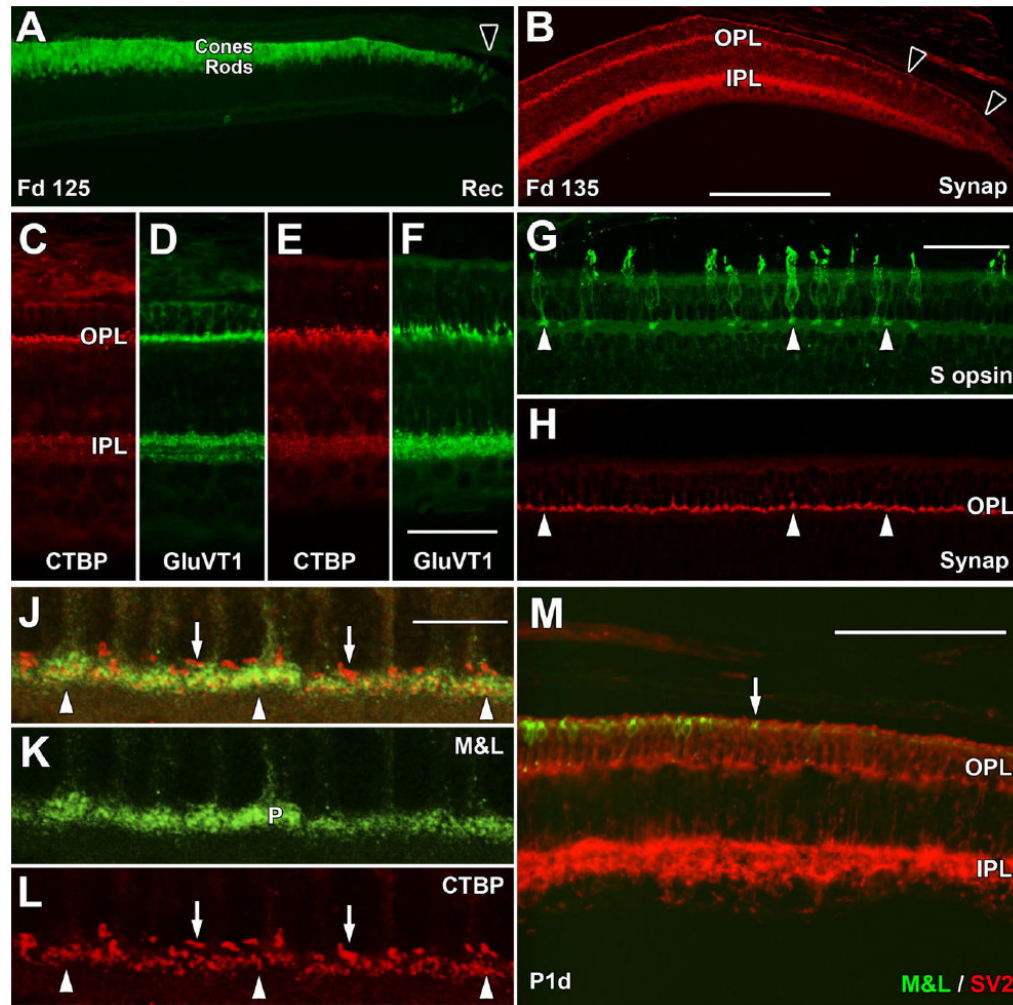
Figure 6.
Late fetal and postnatal expression of synaptic markers. **A:** The far periphery of the Fd 125 retina contains a single layer of Rec+ cones and multiple deep Rec+ rods. Rec labeling extends to the edge of the retina (arrowhead). **B:** The far periphery at Fd 135 has Synap labeling in the IPL to the retinal edge (right arrowhead). In the OPL, there is a dense band of Synap+ cone pedicles, but these become sparse beyond the left arrow. **C–F:** By Fd 135, CTBP2 and GluVT1 prominently label the OPL and IPL in central (C,D) and far peripheral (E,F) retina. **G,H:** At Fd 135, cone pedicles of peripheral S+ cones (G, arrows) label for Synap (H, arrows), as do unlabeled M&L+ cones. **J–L:** Confocal images of central Fd 135 retina showing green M&L+ cone pedicles (J,K) and red CTBP2+ synaptic ribbons (J,L). The cone pedicles contain many thin short ribbons (arrowheads), whereas single, long, thicker ribbons occupy unlabeled spaces above the cone pedicles (arrows), presumably within the rod spherules. **M:** The temporal retinal edge (to the right) at birth has M&L+ cones (arrow) close to, but not at, the edge. SV2+ cones reach the edge, as does the SV2+ labeling in the IPL. A magenta-green copy is available as Supporting Information Figure 2. Scale bars = 200 μm in B (applies to A,B); 50 μm in F (applies to C–F); 50 μm in G (applies to G,H); 10 μm in J (applies to J–L); 100 μm in M.
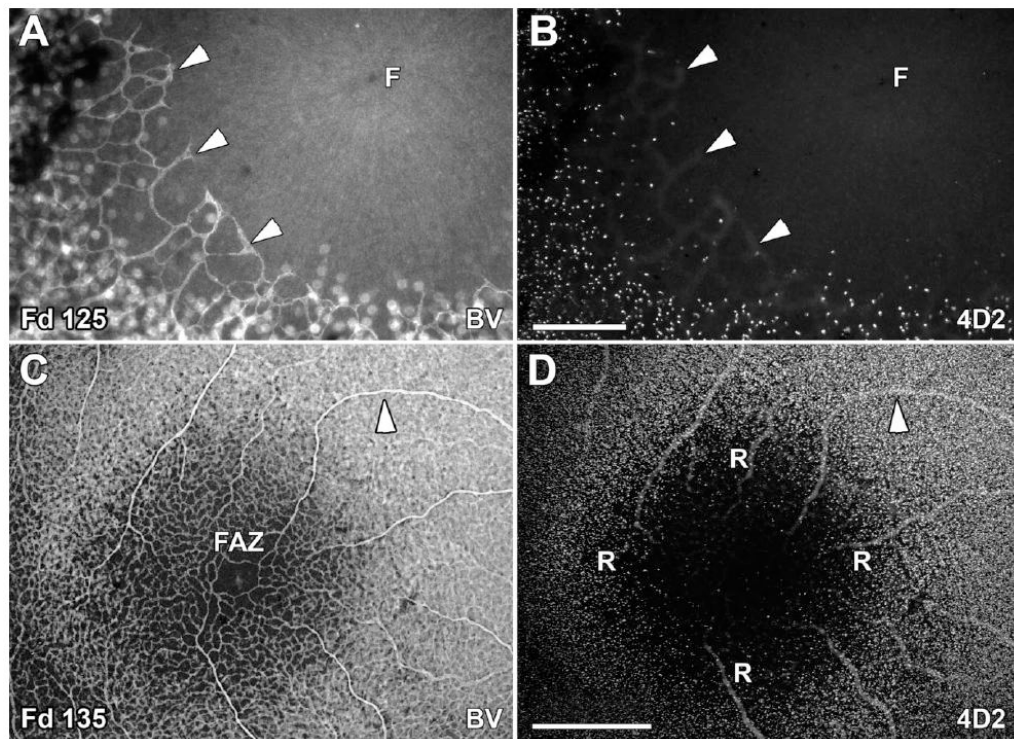
Figure 7.
Relationship of the foveal avascular zone (FAZ) and rods on the foveal edge. **A,B:** At Fd 125, the BV forming the FAZ (A, arrowheads) have not completely encircled the incipient fovea (F). The most central rods (B) overlap the ingrowing BV of the FAZ (arrowheads). **C,D:** By Fd 135, the FAZ is smaller and surrounded by a complete BV ring ~200 μm in diameter (C). In contrast, the rod-free zone (R) is 900 μm wide (D) and is similar in diameter to that seen on Fd 125. The same BV is marked with an arrowhead for orientation. Scale bars = 100 μm in B (applies to A,B); 500 μm in D (applies to C,D).
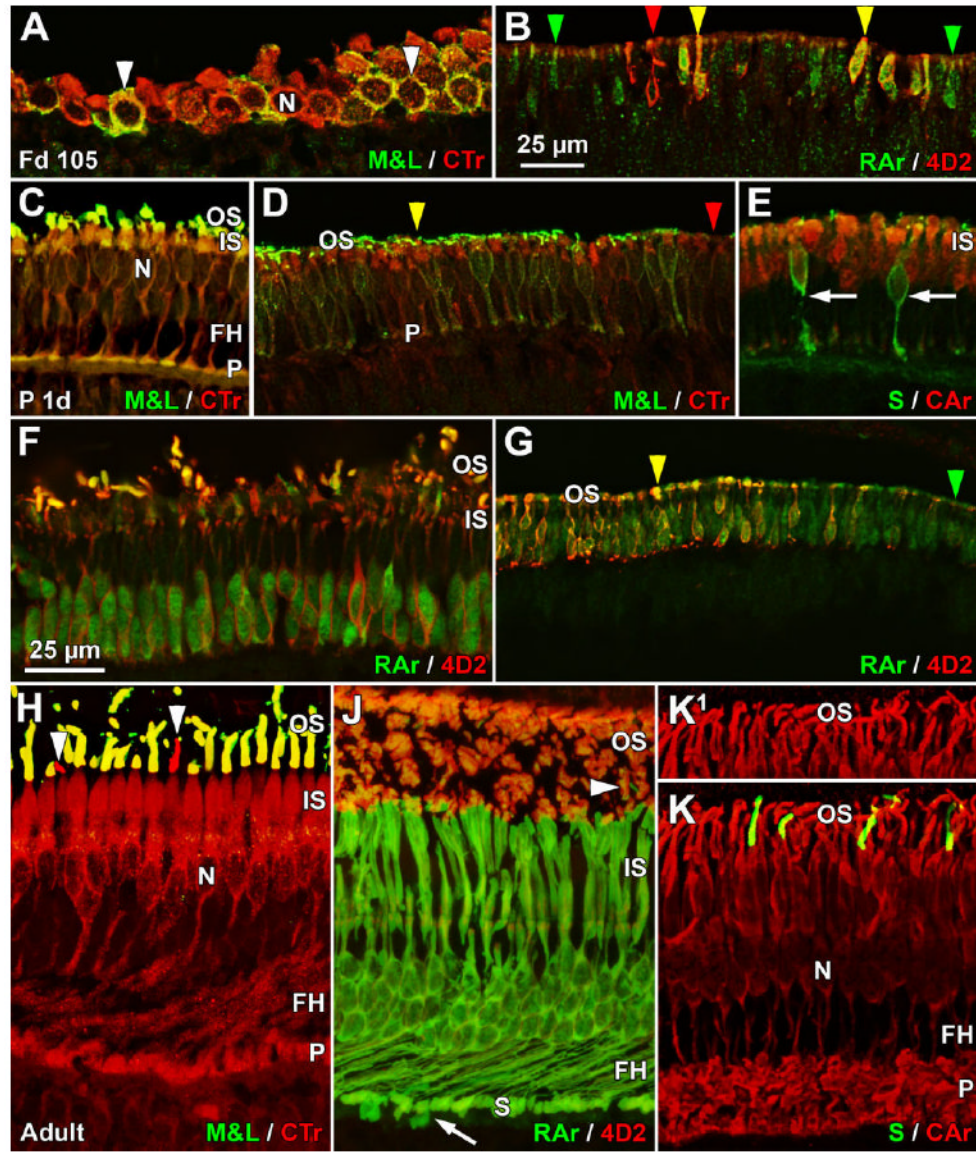
Figure 8.
Confocal images of the expression of phototransduction proteins in marmoset retina. A,B: Fd 105; C–G: neonatal; H–K: 3 months or older. **A:** Tangential section through Fd 105 foveal cones showing membrane labeling for M&L opsin and cytoplasmic labeling for cone transducin (CTr). All cones are CTr$^+$, and a few also are M&L$^+$ (arrowheads). The large nuclei (N) are negative for both proteins. **B:** Labeling at the Fd 105 expression front for 4D2 and rod arrestin (RAr) shows that many rods are RAr$^+$ (green arrowheads), some are RAr$^+$/4D2$^+$ (yellow arrowheads), and a few are 4D2$^+$ (red arrowheads). **C:** At birth, foveal cones have significant CTr labeling throughout the cytoplasm from inner segment (IS) to synaptic pedicle (P) and lighter labeling of the M&L$^+$ outer segment (OS). FH and the pedicles are M&L$^+$/CTr$^+$. **D:** A section 1 mm from the temporal edge of the P3d retina showing that M&L$^+$/CTr$^+$ cones (yellow arrowhead) are close to, but have not reached, the retina edge (to the right), whereas CTr$^+$ cones (red arrowhead) extend to the edge. **E:** Most central neonatal cones, presumably M&L$^+$, show heavy cell body and IS cytoplasmic and lighter nuclear labeling for cone arrestin (CAr). Synaptic pedicles and FH are very lightly labeled. Two S$^+$

cones (arrows) are negative for the mab 7G6 used to detect CAr. **F:** Central neonatal rods have 4D2$^+$ cell membranes and RAr$^+$ nuclei and cytoplasm. All rod OS are heavily 4D2$^+$, and a few rod OS are doubly labeled, whereas IS are 4D2$^+$. **G:** The temporal edge of the P2d retina (to the right), with a narrow band of RAr$^+$ rods (red arrowhead) at the edge and 4D2$^+$/RAr$^+$ rods (yellow arrowhead) slightly more central. **H:** CTr labeling is present throughout the adult cone cytoplasm, but the **N** is negative. M&L$^+$ cones are doubly labeled from OS to P, whereas two S$^+$ OS (arrowheads) are CTr$^+$, indicating that both types of cones contain transducin recognized by the mab A1.1. **J:** Central adult rods have heavy cytoplasmic labeling for RAr, including their FH and synaptic spherule (S). Two deeper cone pedicles, presumably S cones (arrow), are also RAr$^+$. Rod OS are heavily 4D2$^+$ and lightly RAr$^+$, and one short OS (arrowhead), presumably an S cone, is RAr$^+$. **K,K1:** At P3 months, central cones show increased cytoplasmic CAr labeling, including the P, but nuclear labeling has disappeared. A comparison of K and K1 shows that four S$^+$ OS are labeled for CAr as well as surrounding M&L OS. A magenta-green copy is available as Supporting Information Figure 3. Scale bars = 25 μm in B (applies to B,D,G); 25 μm in F (applies to A,C,E,F,H–K).

TABLE 1

Antibody Description and Parameters

Antibody	Working dilution	Immunogen	Source
Mouse anti-CD31	1/50	Human spleen cell membranes	DAKO M0823, Santa Barbara, CA
Mouse anticone arrestin (7G6)	1/250	*Macaca* monkey retinal extract	P. MacLeish, Morehouse University, Atlanta, GA
Mouse anticone transducin (A1.1)	1/200	Amino acids 159–170 of human alpha subunit	J. Hurley, University of Washington, Seattle, WA
Mouse anti-C terminal binding protein 2	1/8,000	C terminal amino acids 361–445 of mouse CTBP2	BD Biosciences 612044, Heidelberg, Germany
Rabbit antiglutamate vesicular transporter 1	1/10,000	Amino acids 456–560 of rat GluVT1	Synaptic Systems 135302, Gottingen, Germany
Rabbit antimedium- and long-wavelength-selective cone opsin	1/5,000	carboxy terminal 18 amino acids of human M opsin	J. Saari, University of Washington, Seattle, WA
Rabbit antirecoverin	1/20,000	Recombinant human protein	Chemicon AB5585, Temecula, CA
Mouse antirhodopsin (4D2)	1/250	Rat outer segments	R. Molday, University of British Columbia, Vancouver, Canada
Rabbit antirod arrestin (C10C10)	1/1,000–1/5,000	Amino acids 287–296 of bovine arrestin 1	C. Craft, University of Southern California, Los Angeles, CA
Rabbit antishort-wavelength-selective cone opsin (JH455)	1/15,000	C terminal amino acids 1–48 of human S cone opsin	J. Nathans, Johns Hopkins University, Baltimore, MD
Mouse antisynaptic vesicle protein 2	1/1,000	*Torpedo* synaptic vesicles	K. Buckley, Harvard Medical School, Boston, MA
Mouse antisynaptophysin	1/1,000	Rat retina synaptosomes	Sigma-Aldrich S5768, St. Louis, MO